

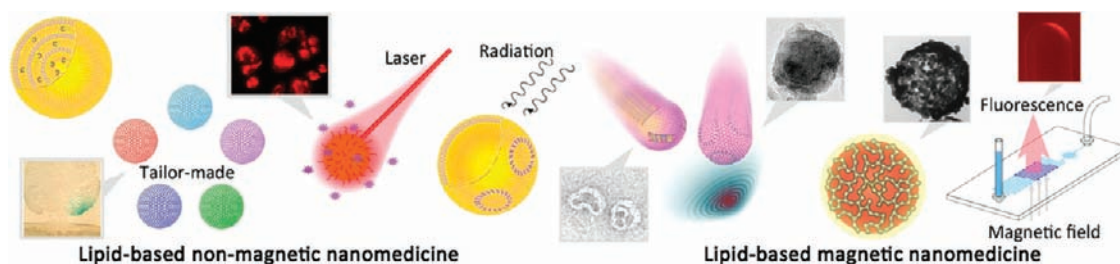
## Nanomedicine for Cancer: Lipid-Based Nanostructures for Drug Delivery and Monitoring<sup>†</sup>

YOSHIHISA NAMIKI,<sup>\*,‡</sup> TERUAKI FUCHIGAMI,<sup>§</sup> NORIO TADA,<sup>‡</sup>  
RYO KAWAMURA,<sup>§</sup> SATOSHI MATSUNUMA,<sup>||</sup>  
YOSHITAKA KITAMOTO,<sup>§</sup> AND MASARU NAKAGAWA<sup>⊥</sup>

<sup>‡</sup>*Institute of Clinical Medicine and Research, The Jikei University School of Medicine, 163-1 Kashiwa-shita, Kashiwa, Chiba, 277-8567, Japan,* <sup>§</sup>*Department of Innovative and Engineered Materials, Tokyo Institute of Technology, J2-40, 4259 Nagatsuta, Midori-ku, Yokohama, 226-8502, Japan,* <sup>||</sup>*Research and Development Division, Hitachi Maxell, 1-1-88 Ushitora, Ibaraki, Osaka, 567-8567, Japan,* and <sup>⊥</sup>*Institute of Multidisciplinary Research for Advanced Materials, Tohoku University, 2-1-1 Katahira, Aoba-ku, Sendai, 980-8577, Japan*

RECEIVED ON JANUARY 19, 2011

### CONSPECTUS



Recent advances in nanotechnology, materials science, and biotechnology have led to innovations in the field of nanomedicine. Improvements in the diagnosis and treatment of cancer are urgently needed, and it may now be possible to achieve marked improvements in both of these areas using nanomedicine. Lipid-coated nanoparticles containing diagnostic or therapeutic agents have been developed and studied for biomedical applications and provide a nanomedicine strategy with great potential. Lipid nanoparticles have cationic headgroups on their surfaces that bind anionic nucleic acids and contain hydrophobic drugs at the lipid membrane and hydrophilic drugs inside the hollow space in the interior. Moreover, researchers can design nanoparticles to work in combination with external stimuli such as magnetic field, light, and ionizing radiation, which adds further utility in biomedical applications.

In this Account, we review several examples of lipid-based nanoparticles and describe their potential for cancer treatment and diagnosis. (1) The development of a lipid-based nanoparticle that included a promoter–enhancer and transcriptional activator greatly improved gene therapy. (2) The addition of a radiosensitive promoter to lipid nanoparticles was sufficient to confer radioisotope-activated expression of the genes delivered by the nanoparticles. (3) We successfully tailored lipid nanoparticle composition to increase gene transduction in scirrhous gastric cancer cells. (4) When lipophilic photosensitizing molecules were incorporated into lipid nanoparticles, those particles showed an increased photodynamic cytotoxic effect on the target cancer. (5) Coating an Fe<sub>3</sub>O<sub>4</sub> nanocrystal with lipids proved to be an efficient strategy for magnetically guided gene-silencing in tumor tissues. (6) An Fe<sub>16</sub>N<sub>2</sub>/lipid nanocomposite displayed effective magnetism and gene delivery in cancer cells. (7) Lipid-coated magnetic hollow capsules carried aqueous anticancer drugs and delivered them in response to a magnetic field. (8) Fluorescent lipid-coated and antibody-conjugated magnetic nanoparticles detected cancer-associated antigen in a microfluidic channel.

We believe that the continuing development of lipid-based nanomedicine will lead to the sensitive minimally invasive treatment of cancer. Moreover, the fusion of different scientific fields is accelerating these developments, and we expect these interdisciplinary efforts to have considerable ripple effects on various fields of research.

## 1. Introduction

The coming together of a variety of scientific disciplines has accelerated the development of applied medicine as a bridge between basic science and clinical practice. Over the past several decades, advances in nanotechnology, materials science, and biotechnology have come together to give rise to the innovative field of nanomedicine. Among the advances which have occurred, nanoparticles have been rapidly developed for the detection and treatment of various diseases.<sup>1</sup> At the same time, cancer is a major cause of death worldwide and is on the increase, and its clinical outcome remains poor. Nanoparticles may have a special utility in this complex, often intractable disease.

As a minimally invasive, reliable, and high-performance medical technology, the sensing and the delivery of cancer-targeted nanomedicines and the monitoring of their distribution are urgently required. The advantages of nanomedicines are as follows: (1) biodistribution can be controlled by the change of the nanoparticle properties, (2) “stealth type nanoparticles” are able to maintain an effective blood concentration by escaping the removal carried out by the reticuloendothelial system (RES), (3) high potency hydrophobic compounds can be dispersed in water and delivered systemically by nanoparticles, and (4) nanoparticles can enhance the level of signal detection for the more sensitive detection of disease.

To date, numerous types of drug delivery systems (DDS) have been developed for cancer treatment, and lipid nanoparticles have been considered one of the most promising options. The history of the development is longer, and clinical trials have been performed more frequently using lipid nanoparticles than other types of nanoparticles.

In this Account, we present various examples of lipid-based nanomedicines for cancer which we have developed (Figure 1). Some of them exert their effect in combination with external energy sources.

## 2. Lipid-Based Nanomedicines for Cancer

The liposome is the oldest<sup>2</sup> and the most common type of lipid-based nanostructure used for biomedical applications. Liposomes have the advantage of being able to contain hydrophobic drugs at the lipid bilayer itself and hydrophilic drugs inside the lipid bilayer, and furthermore, cationic liposomes electrostatically bind anionic nucleic acids to their surface. In this section, we describe liposome-mediated nanomedicines for the treatment of cancer.

**2.1. A Potent Expression System for the Enhancement of Liposome-Mediated Gene Transduction.** Here we describe how the combination of a potent promoter–enhancer with a transcriptional activator greatly enhanced the gene therapeutic effect in cancer treatment.<sup>3</sup> Enhancement of exogenous gene expression is a matter of considerable importance, especially for the success of cancer gene therapy using nonviral vectors, because the transfection efficiency is frequently inadequate. Among the nonviral vectors, cationic liposomes have the advantages of easy preparation and a lack of unacceptable virus-associated adverse reactions, such as the activation of oncogenes.<sup>4</sup> To enhance liposome-mediated gene transduction, we developed cationic multilamellar vesicle (MLV) liposomes containing a potent expression promoter–enhancer and transcriptional activator high mobility group 1,2 (HMG-1,2) chromatin proteins (Figure 2B). This gene therapy vector was examined in combination with cytokines in a metastatic breast cancer nude mouse model. We initially confirmed that the HMG-1,2 protein enhanced the expression of reporter genes by approximately 2-fold under optimal *in vitro* study conditions (data not shown). Subsequently, we monitored the gene distribution at the most effective dose and the ratio of liposome/plasmid deoxyribonucleic acid (DNA)/HMG-1,2 protein, and found that potent luciferase activity was detected only in the tumor tissues (Figure 2C, D). In the treatment study, the liposomes containing tumor necrosis factor- $\alpha$  (TNF- $\alpha$ )-expressing pcagTNF- $\alpha$  prolonged median survival, an effect which was enhanced in combination with interferon- $\gamma$  (INF- $\gamma$ ) (Figure 2E).

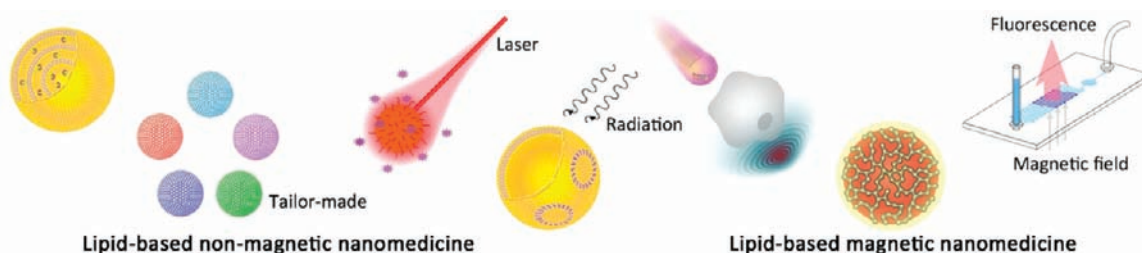


**FIGURE 1.** Diagram of the strategy of lipid-based theranostic nanomedicines for cancer.

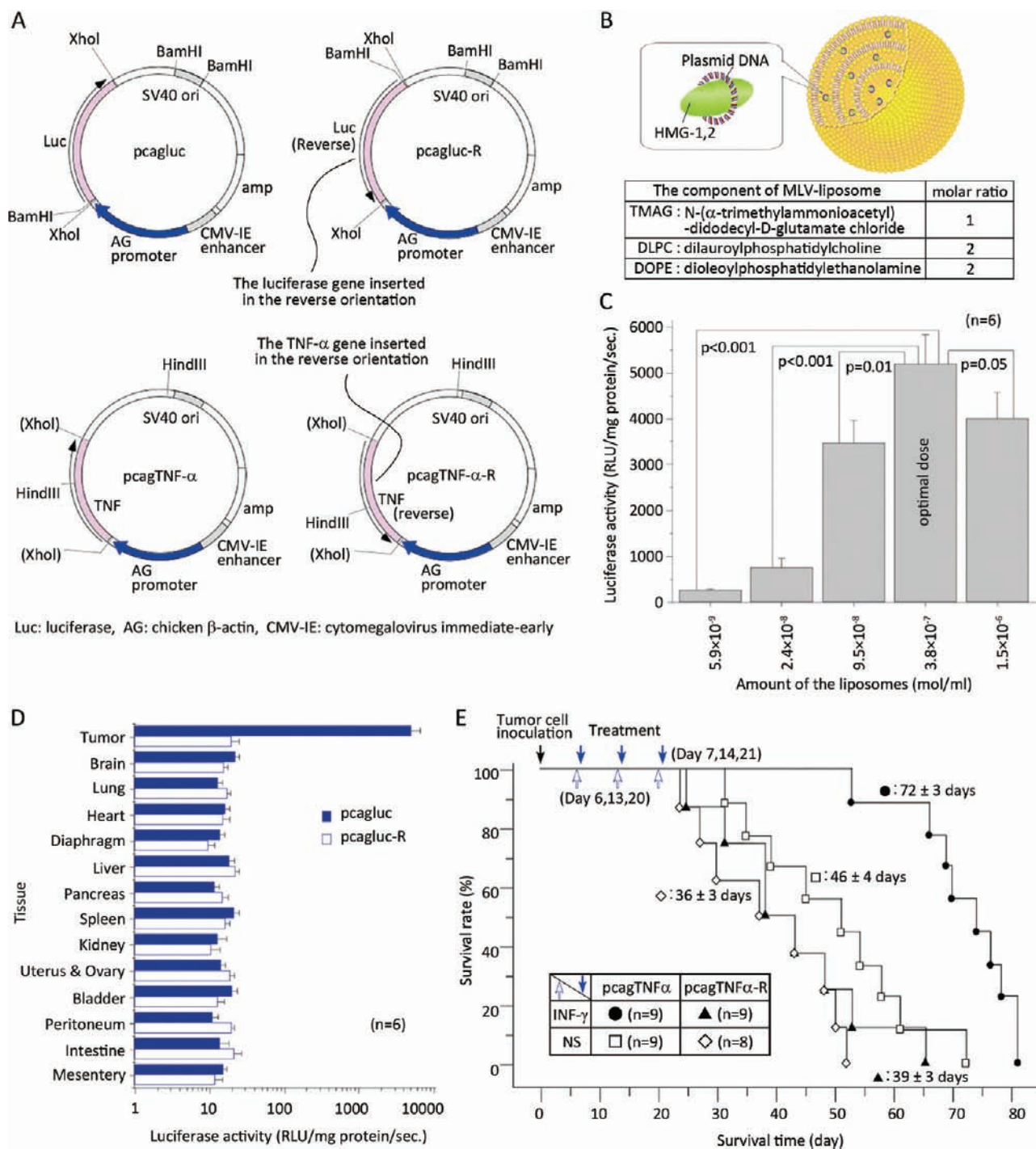


**FIGURE 2.** (A) Plasmid DNAs. (B) Diagram of cationic MLV liposomes containing plasmid DNA and the HMG-1,2 protein. (C) Optimization of the liposome dose for the maximum transfection activity. Mice were intraperitoneally administered liposomes on day 21, including the luciferase-expressing pcagLuc, and the luciferase activity in tumor tissues was examined on day 23. (D) Monitoring of the reporter gene expression in each tissue. Mice were administered the liposomes ( $3.8 \times 10^{-7}$  mol) containing pcagLuc. (E) Treatment in a metastatic breast cancer model. Mice were intraperitoneally given INF- $\gamma$  (4000 U; white arrows) and the liposomes ( $3.8 \times 10^{-7}$  mol) containing pcagTNF- $\alpha$  (blue arrows). (C-E) MCF-7 cells ( $7.5 \times 10^6$ ) were intraperitoneally inoculated into the mice on day 0. Mice were intraperitoneally given liposomes constructed with a cationic lipid (10  $\mu$ mol) including the plasmid DNA (300  $\mu$ g) and the HMG-1,2 protein (96  $\mu$ g). Reproduced in part from ref 3. Copyright 1998 Stockton Press.

These results demonstrate that cationic liposome-mediated gene therapy using a potent expression system is a useful approach to metastatic tumors. As a practical

nanomedicine treatment for cancer, the enhancement of cationic liposomal gene expression obtained by the application of a strong promoter–enhancer combined



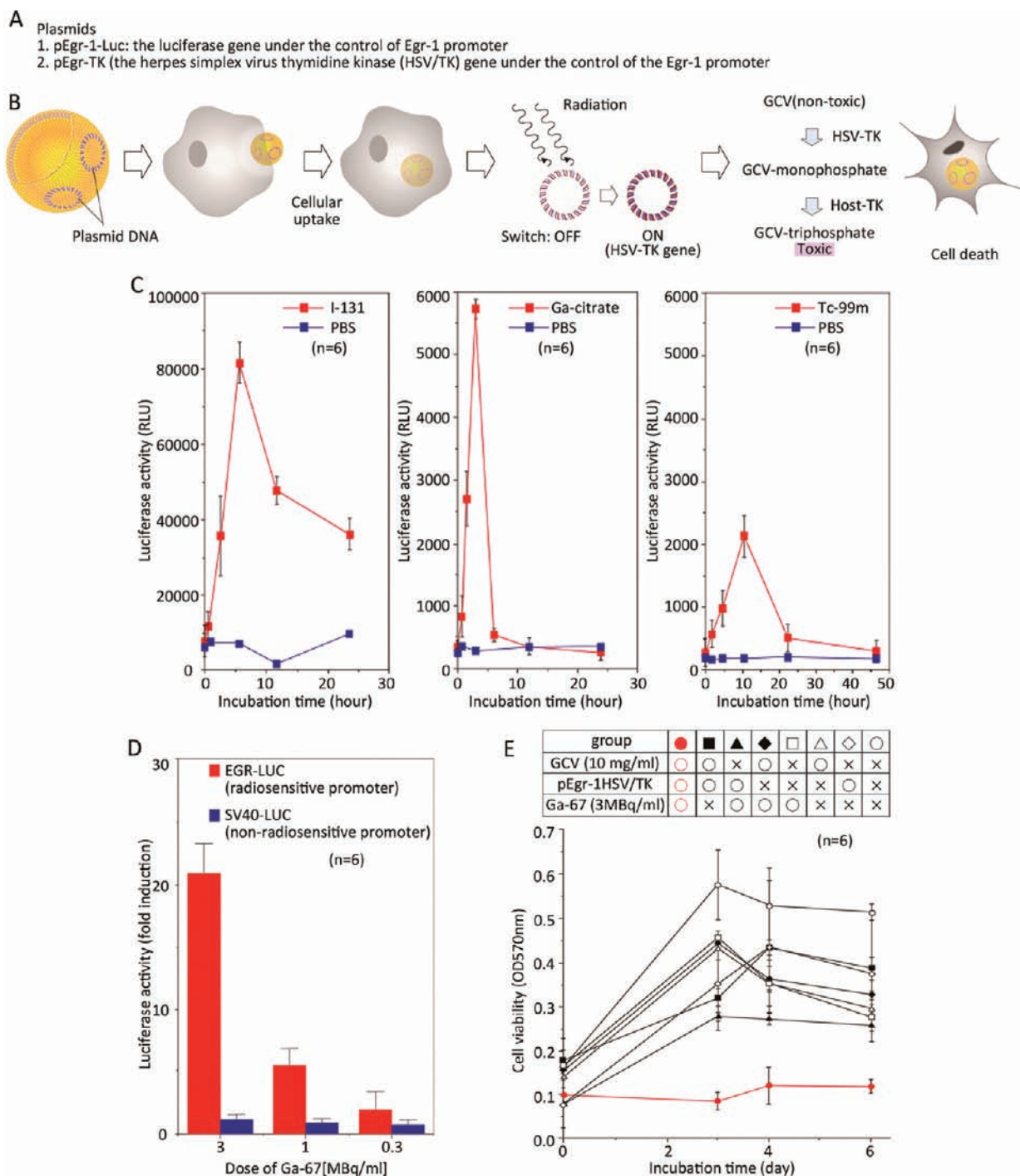


**FIGURE 3.** (A) Plasmid DNAs. (B) Diagram of radioisotope-controlled suicide gene transduction. (C) Time dependent activation of the Egr-1 promoter with radioisotopes. The luciferase activity of the pEgr-Luc-transfected cells incubated with I-131, Ga-67, or Tc-99 m. (D) Dose-dependent activation of Egr-1 transcription by Ga-67. Ga-67-citrate was added to the cells transfected with each plasmid. Luciferase activity was measured at 3 h after irradiation and is displayed as the fold induction. (E) Viability of the pEgr-TK-transduced cells treated with Ga-67 and GCV. The pEgr-Tk-transduced cells were seeded on day 0 and were incubated with Ga-67-citrate. After 15 min, GCV was added to the cells. Cell viability was assessed with MTT cytotoxic assay. (C–E) AsPC-1 cells ( $3 \times 10^4$ ) were tested. Reproduced in part from ref 5. Copyright 1997 Mary Ann Liebert, Inc.

with a transcriptional activator continues to develop, and the strong points, such as nonvirus-method-associated safety, will outweigh the drawback of low transfection efficiency.

**2.2. Radioisotope-Controlled Liposome-Mediated Transduction of the Suicide Gene.** Here we discuss the potential of “radioisotope-controlled” gene transduction as a cancer nanomedicine.<sup>5</sup> Target-specific gene expression is also an issue

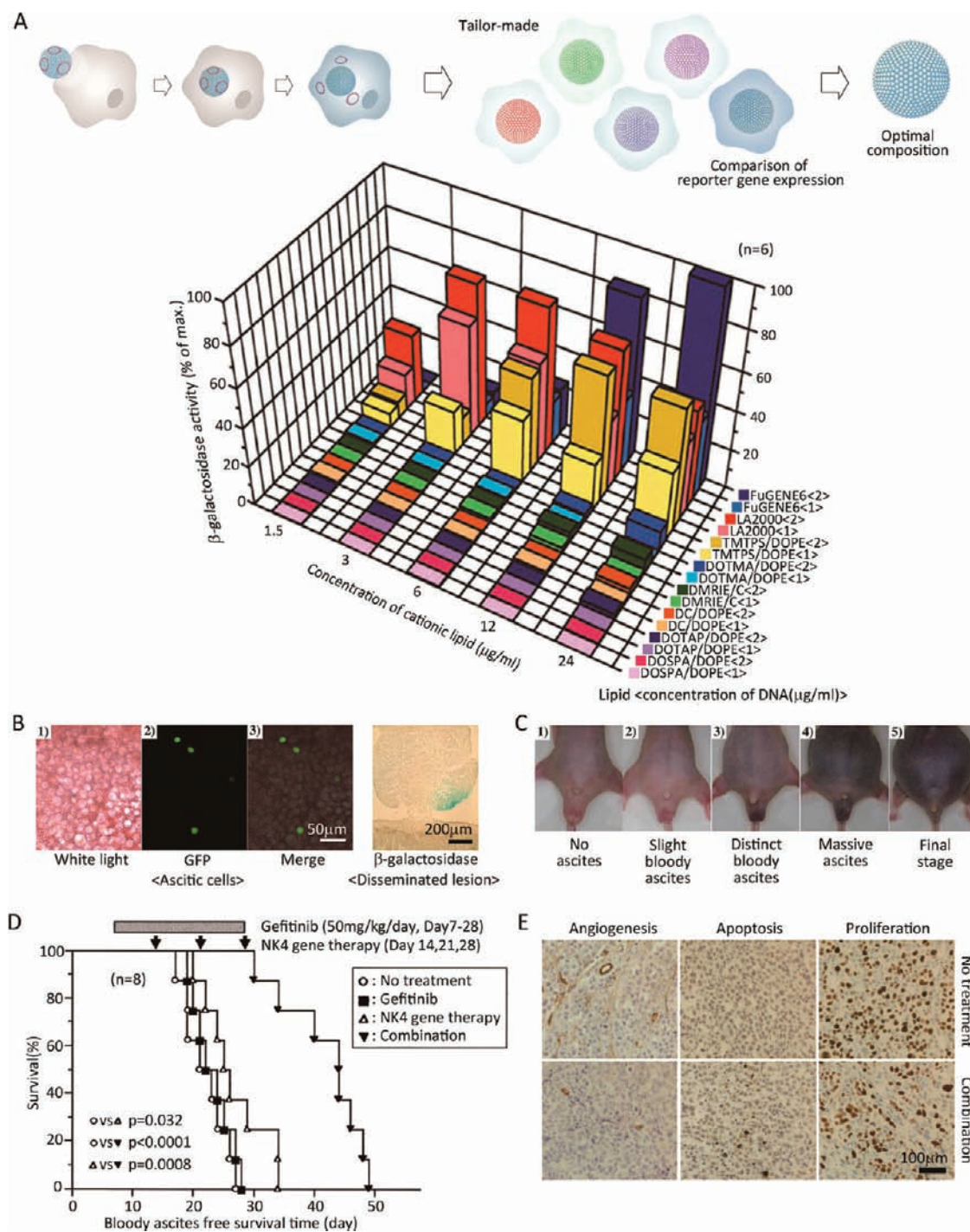


**FIGURE 4.** (A) Optimization of the cationic liposome/DNA complexes in NUGC-4. NUGC-4 cells were incubated with the various types of the  $\beta$ -galactosidase-expressing cationic liposome (1.5–24  $\mu\text{g/ml}$ )/pCMV-SPORT $\beta$ -gal (1 or 2  $\mu\text{g/ml}$ ) complexes, and  $\beta$ -galactosidase activity was compared. (B) Reporter gene expression in the ascitic cells (small red cells, red blood cells; large clear cells, NUGC-4) and the disseminated lesions. Nude mice received the GFP-expressing LA2000 (6  $\mu\text{g}$ )/pCDNA3.1 CT-GFP (2  $\mu\text{g}$ )/HMG-1, 2 (1.28  $\mu\text{g}$ ) complex (1 mL) on day 21. On day 28, ascitic cells were evaluated using fluorescence microscopy. Mice similarly received 1 mL of the  $\beta$ -galactosidase-expressing LA2000 (6  $\mu\text{g}$ )/pCMV-SPORT $\beta$ -gal (2  $\mu\text{g}$ )/HMG-1, 2 (1.28  $\mu\text{g}$ ) complex on day 21.  $\beta$ -Galactosidase in the disseminated lesions was detected with X-Gal staining on day 28. (C) Development of ascites after the coinoculation of NUGC-4 with NF22. (D) Effects of combination therapy. (E) Immunohistochemical evaluation of the treatment. Twenty-eight days after tumor inoculation, the degree of proliferation, apoptosis, and angiogenesis were compared in another mouse model with the detection of Ki-67, ssDNA, and vWF, respectively. (D, E) Mice were orally administered gefitinib and intraperitoneally received 1 mL of the LA2000 (6  $\mu\text{g}$ )/pCDNA3.1 CT-GFP (2  $\mu\text{g}$ )/HMG-1, 2 (1.28  $\mu\text{g}$ ) complex (negative control) or the NK4-expressing LA2000 (6  $\mu\text{g}$ )/pCDNA3 hNK4 (2  $\mu\text{g}$ )/HMG-1, 2 (1.28  $\mu\text{g}$ ) complex. (C–E) NUGC-4 cells ( $1 \times 10^6$ ) plus NF22 cells ( $2 \times 10^6$ ) were coinoculated on day 0. Reproduced in part from ref 8. Copyright 2005 Wiley-Liss, Inc.

in successful cancer gene therapy. We demonstrated that the radiosensitive early growth response gene 1 promoter (Egr-1) was sufficient to confer radioisotope-activated expression of the therapeutic gene in pancreatic tumor cells.

The early response genes that encode the FOS, JUN, and the Egr families play a major part in early signal transduction following a variety of physical stimuli. Egr-1 transduces early stimulation signals in tissue-protective reactions, such as cell proliferation, growth arrest, and tissue repair. Ionizing radiation induces the formation of reactive oxygen intermediates, which indirectly activate Egr-1 transcription. Prior to our investigation, Weichselbaum et al. transfected the TNF-expressing pEgr-TNF into hematopoietic cells and irradiated them with an external beam to elicit Egr-1 promoter induction.<sup>6</sup> Compared with their approach, ours is more suitable for the irradiation of widespread metastatic lesions, because external beam irradiation is only available for local lesions. To anticipate the irradiation of metastatic lesions, we used radioisotopes that are known to accumulate in tumors.

We confirmed that the Egr-1 promoter yielded strong reporter gene expression in the presence of the radioisotope. The degree of Egr-1-activation by radioisotopes was compared in a human pancreatic tumor cell line, AsPc-1 (Figure 3B). Cells were transfected with pEgr-1-Luc using cationic liposomes and then were exposed to each radioisotope. It was found that Ga-67-citrate, which is commonly employed in tumor scintigraphy,<sup>7</sup> was suitable for the triggering of luciferase gene induction (Figure 3C, D). AsPc-1 cells were then transfected with pEgr-TK. Ganciclovir (GCV), which is selectively phosphorylated by the herpes simplex virus thymidine kinase (HSV/TK) so as to exert cytotoxicity, and Ga-67-citrate were added to the pEgr-TK-transfected cells, and the antitumor effect was then assessed. The pEgr-TK-transfected AsPc-1 cells displayed the cytotoxic effect 2 days after the initiation of the treatment (Figure 3E).

These results indicate that pEgr-TK combined with Ga-67 and GCV is a good candidate for irradiation-controllable gene therapy for cancer using liposomes. As an added precautionary measure, modifications such as a radiosensitive promoter combined with an HSV/TK-sensitive pro-drug may be used so that greater reliability will be conferred on future nanomedical treatments for cancer through an enhanced targeting of the expression of specific genes together with more limited cytotoxicity.

**2.3. Enhancement of Gene Transduction with Tailor-Made Liposomes.** Liposomes of tailor-made composition have been shown to greatly improve gene transduction.<sup>8</sup>

We assessed the effect of NK4-expressing gene therapy using tailor-made liposomes combined with gefitinib in scirrhous gastric cancer (SGC)-bearing animals. Every type of cancer cell has its own particular sensitivity to antitumor agents and transfection activity in response to gene therapy vectors. Therefore, an optimized, tailor-made approach is attractive as a more effective means to achieve disease control. Tailor-made approaches were utilized for both the selection of the gefitinib-sensitive SGC cell lines and the design of the cationic liposomes containing the NK4 gene. NK4 binds to the c-Met receptor without activating it and competitively antagonizes HGF c-Met-mediated biological reactions.<sup>9</sup> Gefitinib is a molecular targeting agent for epidermal growth factor receptor (EGFR) tyrosine kinase.<sup>10</sup> Peritoneal dissemination occurs in the terminal stage of SGC, and there is no effective therapy available, but effective control of SGC dissemination might yield a survival benefit.

We initially assessed the gefitinib-sensitivity of eight SGC cell lines, and five of the cell lines displayed various degrees of sensitivity (data not shown). Subsequently, the composition of liposomes containing an NK4-expressing gene was optimized for maximum transfection activity in the highly gefitinib-sensitive NUGC-4 (Figure 4A). Finally, mice were peritoneally coinoculated with NUGC-4 and scirrhous-associated gastric fibroblasts, NF22, on day 0. In this animal model, fibroblasts accelerated tumor progression (Figure 4C) through a secretion of the growth factors needed by SGC cells, which is similar to the case in SGC patients. Mice were given gefitinib and the NK4-expressing tailor-made liposomes. NK4 suppressed gefitinib resistance through an inactivation of such the required growth factors, and eventually, this tailor-made combination helped to decelerate the cancer progression (Figure 4D) by inhibiting the proliferative, angiogenic, and antiapoptotic effects in tumor tissues (Figure 4E).

This tailor-made approach is potentially useful to the treatment of peritoneal disseminated SGC. If rapid and accurate procedures for determining the optimal nanomedicine compositions prior to become feasible, tailor-made cancer treatments of potent efficacy and minimal adverse side reactions would come into clinical practice.

**2.4. Enhanced Photodynamic Effect on Gastric Cancer of a Photosensitive Stealth Liposome.** Here we discuss a photosensitive stealth liposome (PSSL) with a lipophilic photosensitizer incorporated into its lipid bilayer that enhanced its photoactivity.<sup>11</sup> Among the many water insoluble compounds, lipophilic photosensitizers in particular have potential for enhancing photodynamic therapy (PDT), and



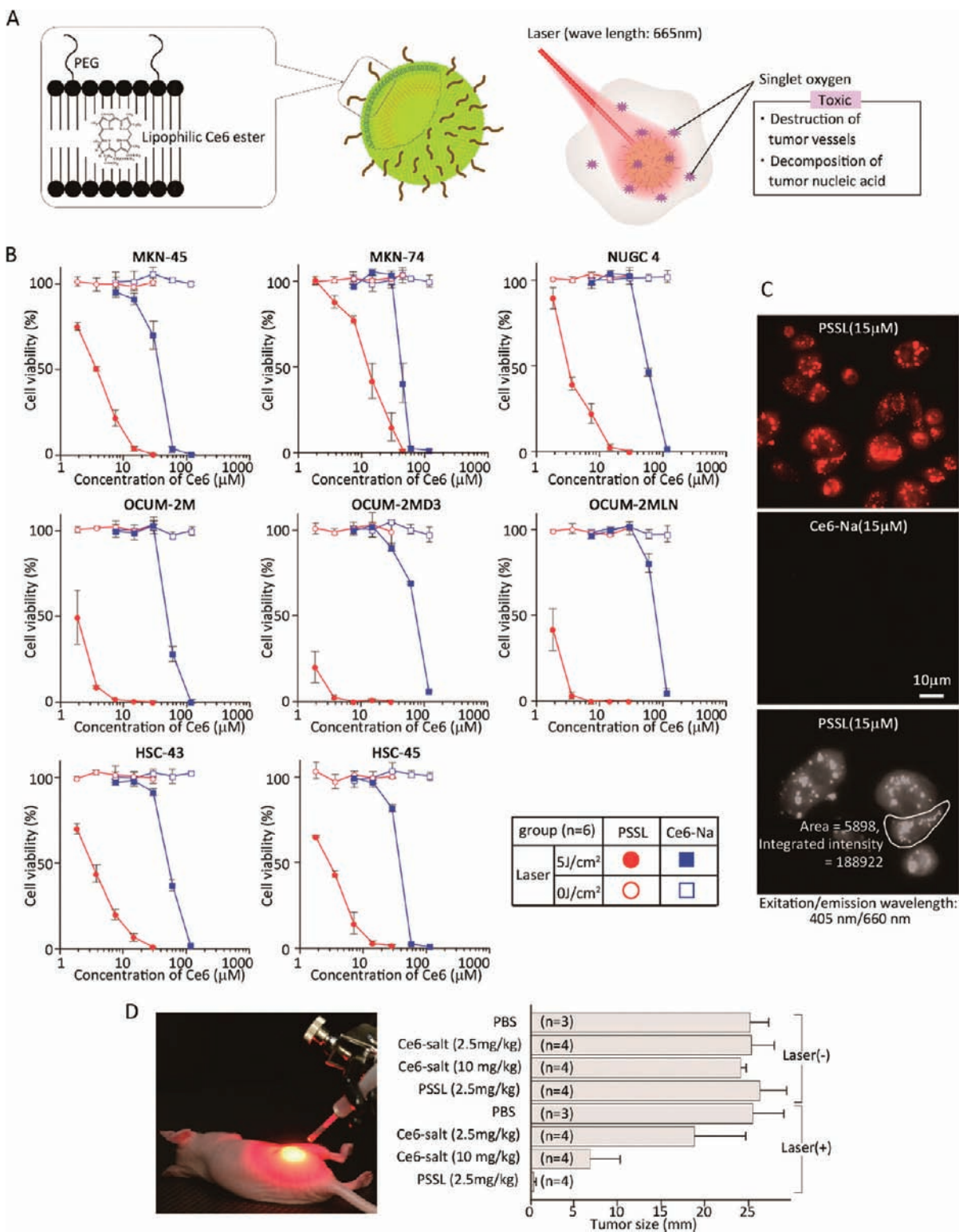


**FIGURE 5.** (A) Diagram of PSSL. PSSL incorporates lipophilic Ce6 ester into its lipid bilayer. (B) Photodynamic effects of PSSL and Ce6–Na in gastric cancer cells. PSSL or Ce6–Na was incubated with each cell line for 30 min, and a laser was used to irradiate them. The cell viability was analyzed by cytotoxic assay after 15 h of laser irradiation. (C) In HSC-45, the cellular uptake (30 min) of PSSL and Ce6–Na was visualized under fluorescence microscopy. The uptake of PSSL by OCUM-2MD3 was semiquantitatively measured. (D) Photodynamic effect of PSSL and Ce6–salt (–Na) in the animal model. HSC-45 cells ( $1 \times 10^6$ ) were subcutaneously inoculated into each nude mouse. When the tumor size reached 12 mm [(the major axis + the minor axis)/2], mice were given 300  $\mu$ L of PBS, Ce6–Na, or PSSL. Two hours later, 100 J/cm<sup>2</sup> of laser light was irradiated onto the tumor. The tumor sizes were compared 20 days after the treatment. Reproduced in part from ref 11. Copyright 2004 Elsevier Ltd.

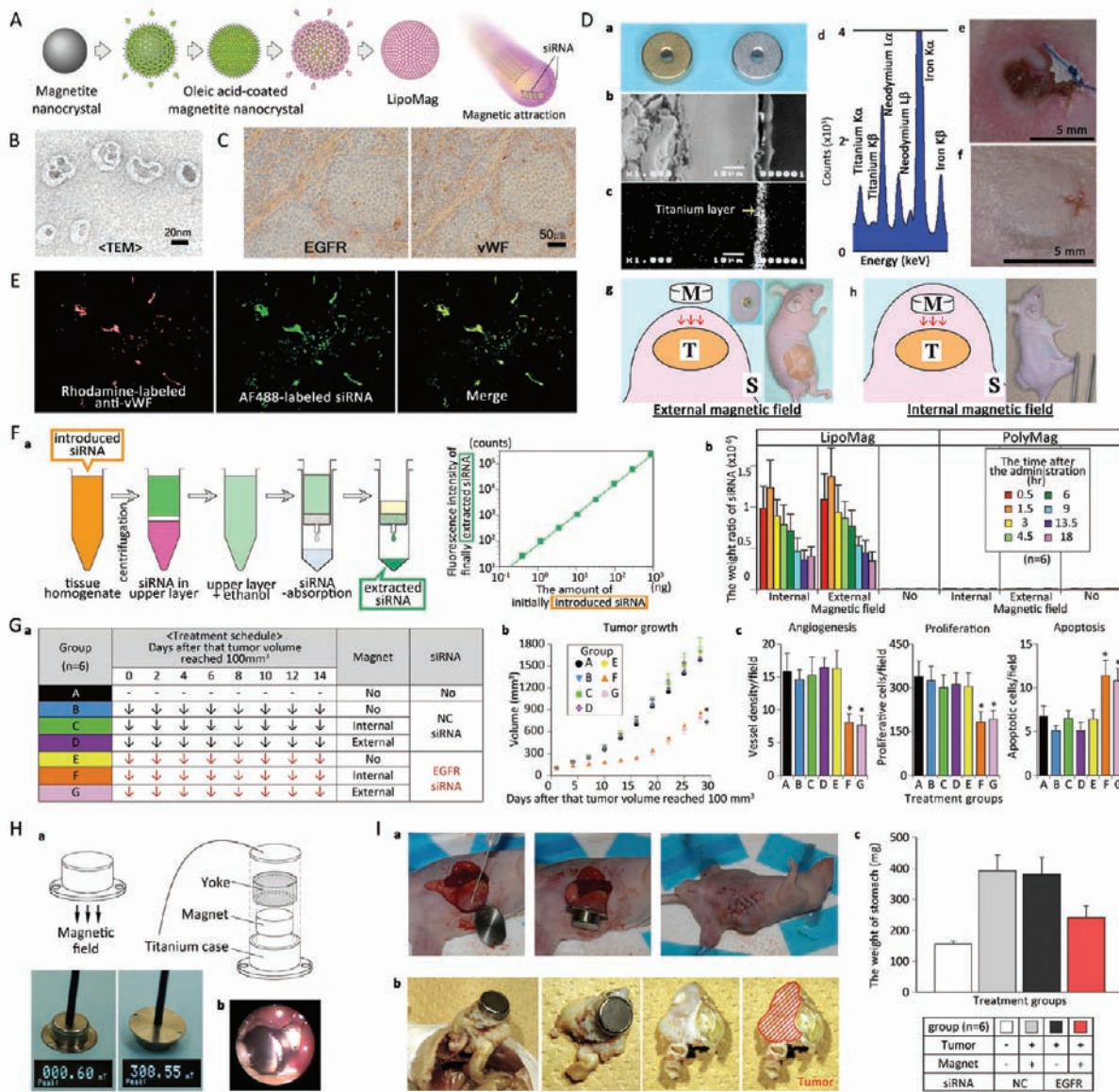


**FIGURE 6.** (A) Diagram of the LipoMag-preparation. (B) Electron micrograph of LipoMag. (C) Immunohistochemical evaluation on serial sections of NUGC-4 xenografts. (D) Metal allergy-free magnets used for the subcutaneous tumor model. (a) Magnets were coated with titanium nitride by an ion plating method (left). Regular nickel-coated magnet (right). Scanning electron micrograph (b) and energy dispersive X-ray analysis (c, d) of the titanium-nitride-coated magnet. (e, f) Allergic inflammation caused by nickel-coated magnets (e) can be avoided with a titanium-coating (f). (g) Titanium-nitride-coated magnet (M) was attached to the tumor lesion (T) over the skin (S) using adhesive tape. (h) A magnet was implanted on tumor tissue under the skin. (E) siRNA distribution in the NUGC-4 xenograft after intravenous administration. (F) Quantification of the bidistributed siRNA. Fluorescence intensity of Alexa Fluor 488 labeled siRNA extracted from the column is proportional to the amount of siRNA introduced into the tissue homogenate. (G) Weight ratio of the siRNA delivered by each vector per NUGC-4 tumor lesion. (H) Antitumor effect of the siRNA<sup>EGFR</sup> delivered by LipoMag in the subcutaneously NUGC-4-inoculated mice. (a) Treatment schedule. (b) Tumor volume for each treatment schedule over time. (c) Two days after the last treatment, the degrees of angiogenesis, proliferation, and apoptosis were compared by immunostaining of vWF, Ki-67, and ssDNA, respectively. \*P < 0.01, compared with group A (no treatment). (I) Diagram and photograph of the magnetic apparatus. (a) A neodymium magnet in the yoke was sealed in a titanium case by gas tungsten arc welding. Strong magnetism was detected on one side of the device using a magnetometer. (b) The biocompatibility of the device sewn onto the gastric wall of healthy mice was confirmed to continue for a period of at least 6 months. (J) Antitumor effect of the siRNA<sup>EGFR</sup> delivered by LipoMag in the orthotopically inoculated gastric cancer model. (a) NUGC-4 cells ( $1 \times 10^6$ ) were inoculated into a site on the outside of the murine gastric wall, and then the magnetic device was sewn onto the wall so as to be fixed at the center of this inoculated region. Mice were administered siRNA<sup>EGFR</sup>/LipoMag at 7, 9, 11, 13, 15, 17, 19, and 21 days after the inoculation with tumor cells. (b, c) Twenty four days after the tumor inoculation, mice were sacrificed and the weight of the stomach in the animals was compared. LipoMag/siRNA (containing 69.1 μg of total lipid and 6 μg of siRNA<sup>EGFR</sup> or siRNA<sup>NC</sup> by per 20 g of mice) was administered. Reproduced in part from ref 13. Copyright 2009 Macmillan Publishers Limited.



water dispersion of lipophilic drugs is one of the important aspects of this approach. PDT<sup>12</sup> is potentially a curative option for early gastric cancer and is also effective even in the advanced stages of gastric cancer cases in areas such as relieving pyloric stenosis. However, porfimer sodium, which is a clinically used photosensitizer, does not specifically accumulate in tumor tissues. The development of a photosensitizer that is accumulated in a sufficient drug concentration in tumor tissues has been urgently awaited. A lipophilic photosensitizer that was reported to have potential in an in vitro study unfortunately also forms large clusters which induce life-threatening thrombosis after intravenous administration, and moreover, these clusters are easily eliminated by the RES with almost no accumulation in tumor tissues.

To examine the possibility of bioapplications of a lipophilic photosensitizer, we prepared PSSL (Figure 5A) and evaluated the in vitro and in vivo photodynamic effects. The prepared PSSL contained polyethylene glycol (PEG) to minimize the recognition and uptake by the RES. In terms of the stealth function, we measured the degree of the escape from the removal by the RES and confirmed that a half to a third less PSSL was removed in murine liver tissues compared with photosensitive nonstealth liposomes (chlorin e6 (Ce6) trimethyl ester/DLPC/DOPE = 1:2:2; molar ratio) 2 h after intravenous administration (data not shown). We compared the photodynamic effects of PSSL with hydrophilic Ce6–Na in gastric cancer cell lines. We found that PSSL had a photocytotoxic effect (80% lethal dose) up to 53 times more potent than Ce6–Na, which had an equivalent molar ratio of the chlorin ring (Figure 5B). At equivalent concentrations of the chlorin ring, a much greater accumulation of drugs was detected in gastric cancer cells in the PSSL group than in the Ce6–Na group (Figure 5C). These results suggest that the enhanced photoactivity may be mainly due to the increased cellular uptake of PSSL.

In animals, when Ce6–Na (2.5 mg/kg) was intravenously given, the therapeutic outcome was insufficient and tumor regrowth occurred within 10 days after PDT. In contrast, implanted tumors were eradicated completely with PSSL (2.5 mg/kg) plus PDT (Figure 5D).

PSSL achieved a striking photoactivity in animal models, and it is evident that PSSL holds promise for PDT against gastric cancer. To develop these technologies, a large number of potential lipophilic compounds which currently are lying idle can easily be changed to the intravenously administrable hydrophilic form, and the maintenance of effective blood concentrations of these therapeutic agents will thus be readily achievable.

### 3. Lipid-Based Magnetic Nanomedicines for Cancer

Magnetic materials provide multiple functions in lipid-based nanomedicine: for example, the magnetic field sensing and the heat generation in an AC magnetic field. In particular, magnetic attraction is potentially utilizable for both the drug delivery and for the disease detection. In this section, we describe the potential utility of lipid-based magnetic nanoparticles as a novel nanomedicine for the treatment and the diagnosis of cancer.

**3.1. Magnetic Crystal-Lipid Nanostructures for Magnetically Guided siRNA Delivery.** Here we describe the utility of lipid-based magnetic nanoparticles as an efficient vector for the RNA interference of cancer.<sup>13</sup> Decomposition of a disease-associated gene using small interfering RNA (siRNA)<sup>14</sup> is a potential approach, but an siRNA delivery that targets lesions successfully remains to be developed.<sup>15</sup> We devised LipoMag, nanoparticles composed of oleic-acid-coated magnetite nanocrystal cores and cationic lipid shells (Figure 6A). Initially, we evaluated the potential of LipoMag as an siRNA transporter in murine gastric tumors after the systemic infusion of LipoMag/fluorescence-labeled siRNA (F-siRNA) and found that fluorescence was detected mainly in the magnetic field-irradiated tumor vessels. We consider the EGFR to be an attractive tumor vessel target, because the overexpression of EGFR was observed in tumor endothelial cells (Figure 6C,E). To monitor the siRNA biodistribution, we sequentially compared the fluorescent intensity of each organ after the systemic infusion of LipoMag/F-siRNA or PolyMag (commercially available polymer-coated magnetic nanocrystals)/F-siRNA. Under a magnetic field, a heavy accumulation of siRNA in tumor lesions was observed only in the LipoMag group (Figure 6F). Moreover, we compared the antitumor effects of the intravenous administration of the tumor vessel-targeted siRNA delivered by LipoMag in the gastric-cancer-inoculated mice. In the subcutaneously inoculated model, LipoMag/siRNA<sup>EGFR</sup> treatment under a magnetic field displayed a 50% greater reduction in tumor volume compared with the control group at the end of the treatment (Figure 6G). However, no significant reduction was observed in the PolyMag groups (data not shown). In the immunohistochemical evaluation, LipoMag/siRNA<sup>EGFR</sup> displayed inhibition of angiogenesis and proliferation, as well as an induction of apoptosis. Finally, using an orthotopically inoculated model, we assessed whether there would be a similar therapeutic effect in more deeply targeted regions. To obtain a target-specific directional magnetic field in deep

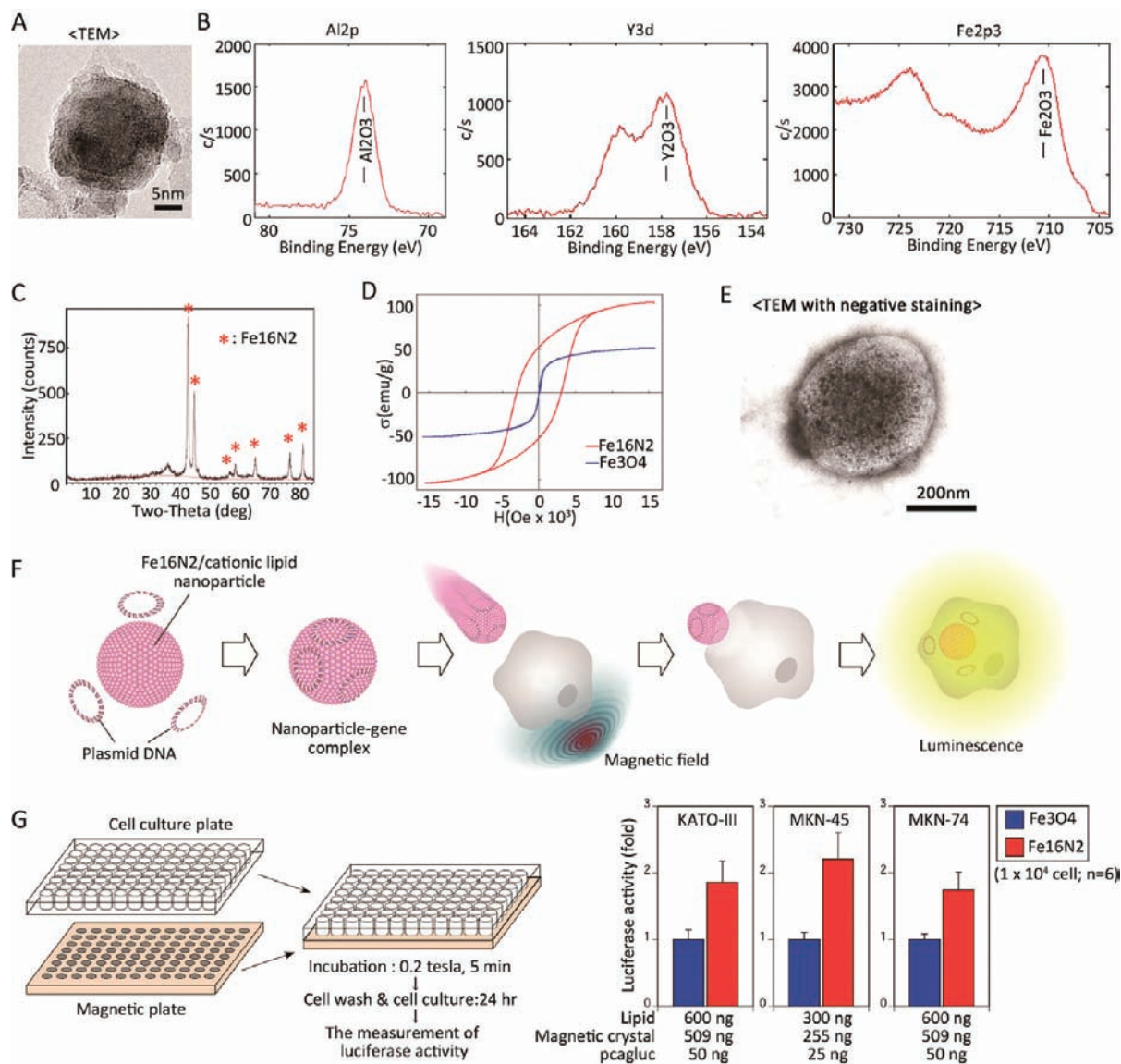


**FIGURE 7.** (A) Electron micrograph of the  $\text{Fe}_{16}\text{N}_2$ /metallic oxide nanocomposite. The average diameter is 26 nm, and the shell thickness is approximately 3.5 nm. (B) The X-ray photoelectron spectroscopy profiles indicated that the metallic oxide shell was composed of aluminum (Al)-, yttrium (Y)-, and iron (Fe)- oxides. These metallic oxides play a role in the prevention of oxidation and decomposition of  $\text{Fe}_{16}\text{N}_2$ . (C) X-ray diffraction peaks originating in  $\text{Fe}_{16}\text{N}_2$  were clearly observed. (D) Magnetization curve of the  $\text{Fe}_{16}\text{N}_2$ /metallic oxide nanocomposite and  $\text{Fe}_3\text{O}_4$ .  $\text{Fe}_{16}\text{N}_2$ /metallic oxide nanocomposite displaying the saturation magnetization (103.1 emu/g) and coercive force (3055 Oe) (cf.  $\text{Fe}_3\text{O}_4$  displayed 50.8 emu/g and 0 Oe). (E) Electron micrograph of the  $\text{Fe}_{16}\text{N}_2$ /cationic lipid nanostructure. (F) Diagram of the expression of a reporter gene transfected with the  $\text{Fe}_{16}\text{N}_2$ /cationic lipid nanostructure. (G) Magnetically guided transfection activity of the  $\text{Fe}_{16}\text{N}_2$ /cationic lipid compared with the  $\text{Fe}_3\text{O}_4$ /cationic lipid in gastric cancer cell lines. Reproduced in part from ref 16. Copyright 2011 Sciyo.

sites within the body, we devised a transplantable magnetic circuit (Figure 6H). For this model, siRNA<sup>EGFR</sup>/LipoMag was administrated and we found that the siRNA<sup>EGFR</sup>/LipoMag group exhibited significantly inhibited tumor growth (Figure 6I).

Overall, tumor-vessel-targeted siRNA delivery using LipoMag combined with transplantable magnets displayed a significant antitumor effect. LipoMag formulations clearly have the potential for widespread use in

tumor-vessel-targeted RNA interference. If an external magnetic field from outside the body can be controlled so as to result in the accumulation of a sufficient amount of magnetic nanoparticles within a targeted lesion, magnetic guidance of siRNA would become a powerful, minimally invasive, and maximally effective delivery system in a variety of diseases.

**3.2. Enhanced Magnetically Guided Gene Transduction Using Iron Nitride Nanocrystal.** The  $\text{Fe}_{16}\text{N}_2$ /cationic

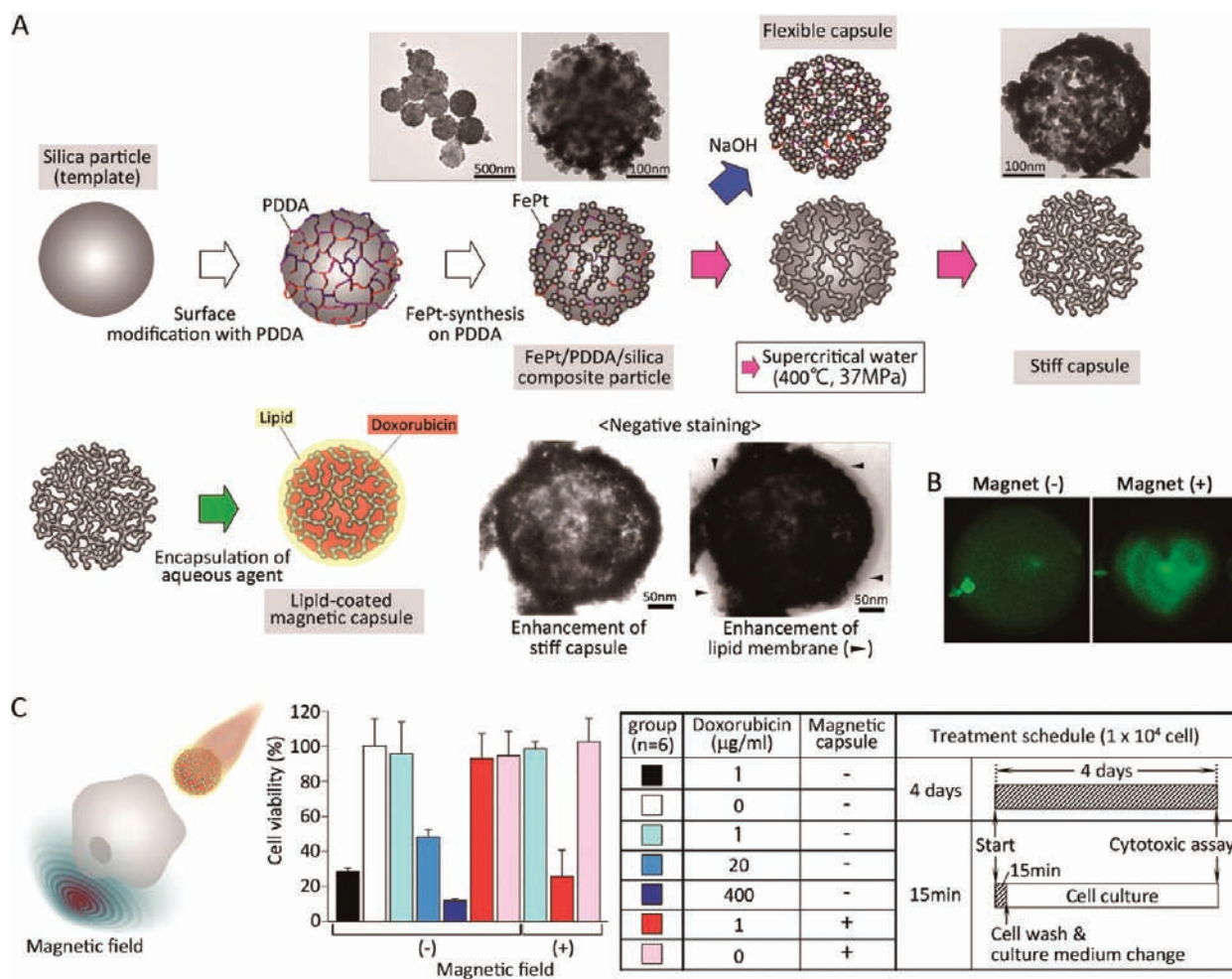


**FIGURE 8.** (A) Diagram of the preparation of the ferromagnetic capsules and the transmission electron micrographs of each synthetic stage. (B) Fluorescence images show the magnetic attraction of the lipid-coated magnetic hollow nanostructure containing aqueous doxorubicin using a heart-shaped magnet. (C) Magnetically (0.2 T) guided cytotoxic effect of the ferromagnetic capsules on a gastric cancer cell line, MKN-45. The amount of doxorubicin entrapped in the ferromagnetic capsules was measured from the fluorescence intensity after the lysis of the nanocomposite membrane with 0.3 N HCL-50% ethanol.<sup>22</sup> (B, C) Excitation/emission wavelength: 510 nm/550 nm. Reproduced in part with permission from ref 19. Copyright 2011 American Chemical Society.

lipid nanocomposite has potential as a gene delivery tool.<sup>16</sup> The iron nitride nanocrystal is an attractive material, not only as a high-density data storage device in the field of information technology<sup>17</sup> but also as a gene therapeutic vector in the field of biomedical technology. For biomedical applications such as gene delivery, iron oxide has been the main magnetic material investigated, while iron nitride nanoparticles have not been previously reported. The magnetic attractive force of magnetic nanoparticles can be enhanced by the optimization of the magnetic materials. Among such materials, Fe<sub>16</sub>N<sub>2</sub> has several advantages, for example: (1) Fe<sub>16</sub>N<sub>2</sub> has a greater degree of magnetization compared with iron oxide, and (2) similar to iron oxide, Fe<sub>16</sub>N<sub>2</sub> is an iron-based biocompatible material, and iron is cheap and abundant.

Both the degree of magnetization and gene therapeutic effect of the magnetic nanocomposite were enhanced by using iron nitride instead of the conventional iron oxide (Figure 7A–D). Initially, we prepared the Fe<sub>16</sub>N<sub>2</sub>/metallic iron oxide nanocomposite, and then the oleic acid-coated Fe<sub>16</sub>N<sub>2</sub>/metallic nanocomposite was assembled with the cationic lipid via hydrophobic interaction<sup>13</sup> (Figure 7E). The obtained magnetic nanoparticles were mixed with the luciferase expressing plasmid DNA, pcagluc, and then electrostatically formed the complexes (Figure 7F). Using the Fe<sub>16</sub>N<sub>2</sub>/cationic lipid nanoparticles, a greater degree of luciferase activity was achieved in the cancer cell lines compared with the Fe<sub>3</sub>O<sub>4</sub>/cationic lipid nanoparticles (Figure 7G).

The development of iron nitride nanoparticles for biomedical needs will ultimately lead to a widespread array of



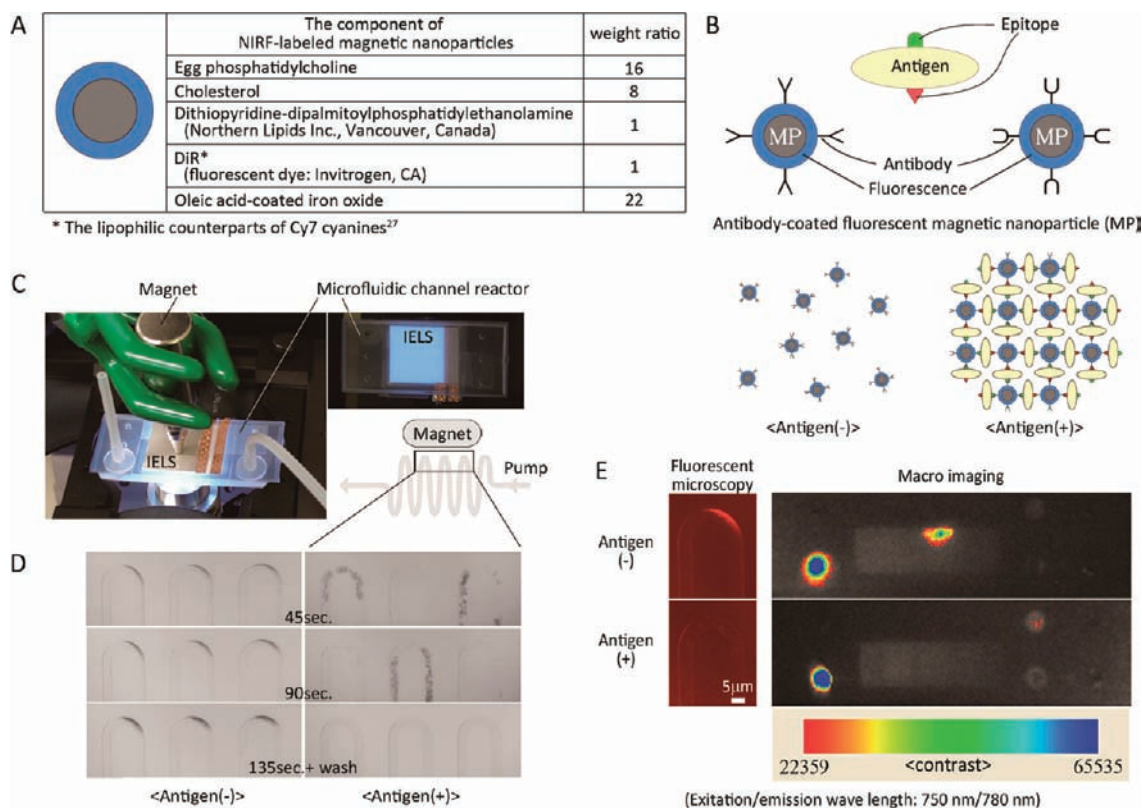


**FIGURE 9.** (A) Fluorescent magnetic nanoparticles. (B) Diagram of the formation of magnetic aggregation resulting from the immune reaction. (C) A magnetic field (0.4 T) was irradiated onto the microfluidic channel reactor over the IELS. Usually, the optical path of the light source is cut off by the magnet attached at the area of interest to the microfluidics. To overcome this problem, we used IELS as the light source of the reactor, because a magnetic field easily passes through the thin IELS (0.3 mm) and reaches the reactor with a minimal loss of magnetism. The constant flow rate (25 nL/min) was generated using a syringe pump (NanoJet, Chemyx Inc. TX). (D) Observation of the immune reaction in the microfluidic channel using the IELS. (E) Detection of the CEA antigen (100 ng/mL) by the absence of the nanoparticle-associated NIRF at the magnetic-field-irradiated region of the microfluidics. A macroimaging system (Lumazone FA with 512BE, Roper Industries, Inc., FL) was used to measure the distribution of fluorescent intensity.

medical applications, including not only target-specific DDS but also the highly sensitive detection of diseases. In addition to iron nitride, there may be a considerable number of other potential magnetic materials for biomedical applications among the industrial magnetic materials, including high-density data storage device applications.

**3.3. Hydrothermal Synthesis of Ferromagnetic Capsules for Aqueous Anticancer Drugs.** Ferromagnetic capsules of several hundred nanometers in diameter having a nanometer-thick shell will be applicable to a magnetically guided DDS of aqueous agents. The porous ferromagnetic nanostructure encapsulates aqueous drugs in the interior hollow space and can be attracted by magnetism. Most of the previous magnetic nanoparticles have had a solid structure composed of a magnetic nanocrystal core and lipophilic drug shell with only limited internal space available for carrying aqueous agents. We have newly devised porous and hollow magnetic capsules which enable the loading

of large amounts of aqueous agents into the cavity (Figure 8A). Initially, a silica particle modified with cationic polymer poly(diaryldimethylammonium chloride) (PDDA) was used as a template for the ferromagnetic capsules. Ferromagnetic FePt nanoparticles were deposited on the surface of the template through a polyol method.<sup>18</sup> An FePt-nanoparticle/PDDA nano-hybrid shell of 5 nm thickness also exhibits ferromagnetic features at room temperature, because the FePt nanoparticles of an ordered-alloy phase are formed with the aid of PDDA despite the small size (3–4 nm). The crystallographic and magnetic properties of the FePt nanoparticles depend on the preparation temperature.<sup>19</sup> Using supercritical water,<sup>20</sup> the silica template is sequentially dissolved after the FePt nanoparticles are thermally fused together on the template. The nanometer-thick network shell is mainly composed of fused FePt nanoparticles and maintains a three-dimensional hollow structure.<sup>21</sup> The mixture of the aqueous anticancer

drug with the dried ferromagnetic capsules was vacuumed to remove air from the hollow space and the space was filled with the aqueous anticancer drug. The surface of the drug-loaded magnetic capsules was then coated with egg phosphatidylcholine to avoid the leakage of the agents. Ultimately, the magnetic attraction of the lipid-coated magnetic capsules (Figure 8B) and the enhanced antitumor effect were derived from magnetic guidance in gastric cancer cells (Figure 8C).

These magnetic hollow capsules enable temporal and spatial modifications, that is, a “four-dimensional” manipulation of a large amount of aqueous drugs by the application of a magnetic field. In the engineering field, both the external and internal large surface area of the porous metallic capsules have potentially far-reaching benefits in applications such as the development of catalysts, fuel cells, and so on.

**3.4. The Diagnosis of Cancer Using Fluorescent Magnetic Nanoparticles and a Microfluidic Channel.** Fluorescent magnetic nanoparticles have potential as a tool in the diagnosis of cancer. Antibody-conjugated magnetic nanoparticles bound to the targeted antigen and formed a large aggregation, which was distinguishable from nonaggregated magnetic nanoparticles by comparing the accumulation pattern under a magnetic field in a microfluidic channel reactor. We synthesized near-infrared fluorescent (NIRF)-labeled magnetic nanoparticles conjugated with anti-carcinoembryonic antigen (CEA) antibodies. The particle surfaces were conjugated with the antibody through a conventional procedure using SPDP and dithiothreitol,<sup>23</sup> and finally the CEA-targeted NIRF magnetic nanoparticles were prepared. The obtained nanoparticles and CEA antigen were mixed to form the aggregation of the antigen–nanoparticle complexes (Figure 9B). This mixture was applied to the entrance of the microfluidic channel reactor,<sup>24</sup> and a magnetic field was irradiated onto the upper region of the microfluidic channel (Figure 9C). In the absence of antigen, nonaggregated nanoparticles were gradually attracted by the magnetic field, but in the presence of antigen the aggregated complexes were hardly entrapped by magnetic field and passed through the microfluidic channel (Figure 9D, E). This result suggests that the driving force of the aggregation generated by the water flow in the narrow space of the microfluidic channel was greater than the magnetic force which attracted the aggregations. The NIRF-labeled magnetic nanoparticles directed at cancer-related antigen and the microfluidic channel are potentially of use as a cancer diagnostic system. Compared with the procedure reported by Degré,<sup>25</sup> the one we used had the following advantages: (1) real time observation of magnetic nanoparticle

movement using an inorganic electroluminescence sheet (IELS)<sup>26</sup> and (2) very low background noise as a result of using NIRF.

Further investigation and together with the eventual optimization of the reaction conditions of the nanoparticles and microfluidic channels will ultimately reveal the clinical utility of this system. As an early diagnostic tool in various diseases, this system has the capacity for rapid and sensitive detection, even from a very limited amount of clinical samples. Moreover, this electroluminescent microfluidic channel will also serve to allow for an analysis of the magnetism directed hydrodynamics of magnetic nanoparticles.

## 4. Conclusion and Perspectives

This Account highlights lipid-based nanoparticles as a cancer-targeted theranostic nanomedicine. The fusion of nanotechnology, materials science, and biotechnology is bringing about advances in the medical technologies used for the diagnosis and treatment of cancer, as well as the monitoring of drug distribution. Lipid-based nanomedicines clearly afford new options in the management of this critically important disease.

For the success of lipid-based nanomedicine, further studies are required. Most importantly, the long-term safety of nanomaterials for *in vivo* applications should be confirmed. It is also necessary to devise a means of mass producing nanoparticles, as well as optimizing their dose or concentration, flow rate, size of the microfluidic channel reactor, and so forth.

Lipid-based nanomedicines have great potential in clinical practice for the purposes of early detection and minimally invasive treatment of cancer, and are expected to bring about an improvement in the detection rate, clinical outcome, and patient quality of life. We believe that the development of nanomedicine will be rapidly accelerated via this fusion of different scientific disciplines and will provide a considerable ripple effect in turn on these disciplines as well.

---

### BIOGRAPHICAL INFORMATION

**Yoshihisa Namiki** received his M.D. (1993) and Ph.D. (1996) in Medicine from the Jikei University School of Medicine. His current research focuses on cancer nanomedicine.

**Teruaki Fuchigami** received his B.Eng. (2009) from Gunma University and M.Eng. (2010) from Tokyo Institute of Technology.

**Norio Tada** received his M.D. (1972) and Ph.D. (1984) in Medicine from the Keio University and the Jikei University School of Medicine, respectively. His current research focuses on lipid metabolism.

**Ryo Kawamura** received his B.S. (2008) from Kitazato University and M.Eng. (2010) from Tokyo Institute of Technology.

**Satoshi Matsunuma** received his B.S. in Chemistry (1983) from the Tokyo University of Science. He obtained his M.S. (1985) and Ph.D. (1988) in Physical Chemistry from Tokyo Institute of Technology. His current research focuses on magnetic beads for bioapplications.

**Yoshitaka Kitamoto** received his B.Eng. (1986), M.Eng. (1988), and Ph.D. (1998) in Electrical and Electronic Engineering from Tokyo Institute of Technology. His current research focuses on magnetic beads for bioapplications.

**Masaru Nakagawa** received his B.Eng. (1992), M.Eng. (1994), and Ph.D. (1997) in Engineering from Sophia University. His current research focuses on monolayer engineering for nanomaterial assembly.

*We would like to acknowledge staff of our respective institutes for their assistance. This work was supported by an Industrial Technology Research Grant (08C46049a) from NEDO of Japan, a Funding Program for Next Generation World-Leading Researchers (LS114) from JSPS and by a Life Science Foundation of Japan. Pacific Edit reviewed the manuscript prior to submission.*

#### FOOTNOTES

\*To whom correspondence should be addressed. E-mail: cancer\_gene\_therapy@ybb.ne.jp.

†We dedicate this work to the late T. Terada and the late K. Nariai.

#### REFERENCES

- Shah, R. B.; Khan, M. A. Nanopharmaceuticals: Challenges and regulatory perspective. In *Nanotechnology in Drug Delivery*; de Villiers, M. M., Aramwit, P., Kwon, G. S., Eds.; Springer: New York, 2009; pp 621–647.
- Bangham, A. D. A correlation between surface charge and coagulant action of phospholipids. *Nature* **1961**, *192*, 1197–1198.
- Namiki, Y.; Takahashi, T.; Ohno, T. Gene transduction for disseminated intraperitoneal tumor using cationic liposomes containing non-histone chromatin proteins. *Gene Ther.* **1998**, *5*, 240–246.
- Montier, T.; Benvegna, T.; Jaffrès, P. A.; Yaouanc, J. J.; Lehn, P. Progress in cationic lipid-mediated gene transfection. *Curr Gene Ther.* **2008**, *8*, 296–312.
- Takahashi, T.; Namiki, Y.; Ohno, T. Induction of the suicide HSVtk gene by activation of the Egr-1 promoter with radioisotopes. *Hum. Gene Ther.* **1997**, *8*, 827–833.
- Weichselbaum, R. R.; Kufe, D. W.; Advani, S. J.; Roizman, B. Molecular targeting of gene therapy and radiotherapy. *Acta Oncol.* **2001**, *40*, 735–738.
- Silver, S. Radioactive isotopes in clinical medicine. *N. Engl. J. Med.* **1965**, *272*, 569–574.
- Namiki, Y.; Namiki, T.; Yoshida, H.; Date, M.; Yashiro, M.; Matsumoto, K.; Nakamura, T.; Yanagihara, K.; Tada, N.; Sato, J.; Fujise, K. Preclinical study of a 'tailor-made' combination of NK4-expressing gene therapy and gefitinib for disseminated peritoneal scirrhous gastric cancer. *Int. J. Cancer* **2006**, *118*, 1545–1555.
- Matsumoto, K.; Nakamura, T. NK4 (HGF-antagonist/angiogenesis inhibitor) in cancer biology and therapeutics. *Cancer Sci.* **2003**, *94*, 321–327.
- Mendelsohn, J.; Baselga, J. The EGF receptor family as targets for cancer therapy. *Oncogene* **2000**, *19*, 6550–6565.
- Namiki, Y.; Namiki, T.; Date, M.; Yanagihara, K.; Yashiro, M.; Takahashi, H. Enhanced photodynamic antitumor effect on gastric cancer by a novel photosensitive stealth liposome. *Pharmacol. Res.* **2004**, *50*, 65–76.
- Dougherty, T. J. Photodynamic therapy of malignant tumors. *Crit. Rev. Oncol. Hematol.* **1984**, *2*, 83–116.
- Namiki, Y.; Namiki, T.; Yoshida, H.; Ishii, Y.; Tsubota, A.; Koido, S.; Nariai, K.; Mitsunaga, M.; Yanagisawa, S.; Kashiwagi, H.; Mabashi, Y.; Yumoto, Y.; Hoshina, S.; Fujise, K.; Tada, N. A novel magnetic crystal-lipid nanostructure for magnetically guided in vivo gene delivery. *Nat. Nanotechnol.* **2009**, *4*, 598–606.
- Fire, A.; Xu, S.; Montgomery, M. K.; Kostas, S. A.; Driver, S. E.; Mello, C. C. Potent and specific genetic interference by double-stranded RNA in *Caenorhabditis elegans*. *Nature* **1998**, *391*, 806–811.
- Toub, N.; Malvy, C.; Fattal, E.; Couvreur, P. Innovative nanotechnologies for the delivery of oligonucleotides and siRNA. *Biomed. Pharmacother.* **2006**, *60*, 607–620.
- Namiki, Y.; Matsunuma, S.; Inoue, T.; Koido, S.; Tsubota, A.; Kuse, Y.; Tada, N. Magnetic nanostructures for biomedical application. In *Nanocrystal*; Masuda, Y., Ed.; Sciyo: Rijeka, Croatia, 2011; in press.
- Sasaki, Y.; Usuki, N.; Matsuo, K.; Kishimoto, M. Development of NanoCAP Technology for High-Density Recording. *IEEE Trans. Magn.* **2005**, *41*, 3241–3243.
- Jeyadevan, B.; Urakawa, K.; Hobo, A.; Chinnasamy, N.; Shinoda, K.; Tohji, K.; Djayaprawira, D. D. J.; Tsunoda, M.; Takahashi, M. Direct synthesis of fct-FePt nanoparticles by chemical route. *J. Appl. Phys.* **2003**, *42*, 350–352.
- Fuchigami, T.; Kawamura, R.; Kitamoto, Y.; Nakagawa, M.; Namiki, Y. Ferromagnetic FePt-nanoparticles/polycation hybrid capsules designed for a magnetically guided drug delivery system. *Langmuir* **2011**, *27*, 2923–2928.
- Ikushima, Y. Supercritical fluids: an interesting medium for chemical and biochemical processes. *Adv. Colloid Interface Sci.* **1997**, *71*, 259–280.
- Namiki, Y.; Kitamoto, Y.; Nakagawa, M.; Fuchigami, T.; Kawamura, R. The preparation of magnetic hollow nanostructures and the drug carrier which contains these nanostructures. International Patent Application PCT/JP2011/000638.
- Gabizon, A.; Dagon, D.; Goren, D.; Barenholz, Y.; Fuks, Z. Liposomes as in vivo carriers of Adriamycin. *Cancer Res.* **1982**, *42*, 4734–4739.
- Barbet, J.; Machy, P.; Leserman, L. D. Monoclonal antibody covalently coupled to liposomes. *J. Supramol. Struct. Cell. Biochem.* **1981**, *16*, 243–258.
- Whitesides, G. M.; Ostuni, E.; Takayama, S.; Jiang, X.; Ingber, D. E. Soft lithography in biology and biochemistry. *Annu. Rev. Biomed. Eng.* **2001**, *3*, 335–373.
- Degré, G.; Brunet, E.; Dodge, A.; Tabeling, P. Improving agglutination tests by working in microfluidic channels. *Lab Chip* **2005**, *5*, 691–694.
- Namiki, Y.; Namiki, T. Electroluminescent disease diagnostic chip. Japanese Patent Application 2009-164711.
- Texier, I.; Goutayer, M.; Da Silva, A.; Guyon, L.; Djaker, N. Cyanine-loaded lipid nanoparticles for improved in vivo fluorescence imaging. *J. Biomed. Opt.* **2009**, *14*, 054005.